Expansion of a lithium gas in the BEC-BCS crossover

J. Zhang[a,b], **E. G. M. van Kempen**[c], **T. Bourdel**[a], **L. Khaykovich**[a,d],
J. Cubizolles[a], **F. Chevy**[a]

M. Teichmann[a] **L. Tarruell**[a], **S. J. J. M. F. Kokkelmans**[a,c], and **C. Salomon**[a]

[a] **Laboratoire Kastler-Brossel, ENS, 24 rue Lhomond, 75005 Paris,**
[b] **SKLQOQOD, Institute of Opto-Electronics, Shanxi University, Taiyuan 030006, P.R. China,**
[c] **Eindhoven University of Technology, P.O. Box 513, 5600 MB Eindhoven, The Netherlands,**
[d] **Department of Physics, Bar Ilan University, Ramat Gan 52900, Israel.**

Abstract

We report on experiments in ^{6}Li Fermi gases near Feshbach resonances. A broad s-wave resonance is used to form a Bose-Einstein condensate of weakly bound ^{6}Li$_2$ molecules in a crossed optical trap. The measured molecule-molecule scattering length of 170^{+100}_{-60} nm at 770 G is found in good agreement with theory. The expansion energy of the cloud in the BEC-BCS crossover region is measured. Finally we discuss the properties of p-wave Feshbach resonances observed near 200 Gauss and new s-wave resonances in the heteronuclear ^{6}Li- ^{7}Li mixture.

Strongly interacting fermionic systems occur in a variety of physical processes, ranging from nuclear physics, to high temperature superconductivity, superfluidity, quark-gluon plasmas, and ultra-cold dilute gases. Thanks to the phenomenon of Feshbach resonances, these gases offer the unique possibility to tune the strength and the sign of the effective interaction between particles. In this way, it is possible to study the crossover between situations governed by Bose-Einstein and Fermi-Dirac statistics.

1 BEC-BCS crossover near ^{6}Li s-wave resonance

When the scattering length a characterizing the 2-body interaction at low temperature is positive, the atoms can pair in a weakly bound molecular state. When the temperature is low enough, these bosonic dimers can form a Bose-Einstein condensate (BEC) as observed very recently in ^{40}K [1] and ^{6}Li [2, 3, 4]. On the side of the resonance where a is negative, one expects the well known Bardeen-Cooper-Schrieffer (BCS) model for superconductivity to be valid. However, this simple picture of a BEC phase on one side of the resonance and a BCS phase on the other is valid only for small atom density n. When $n|a|^3 \gtrsim 1$ the system enters a strongly interacting regime that represents a challenge for many-body theories [5]. In the recent months, this regime has been the subject of intense experimental activity [4, 6, 7, 8, 9, 10, 11].

Here we first report on Bose-Einstein condensation of ^{6}Li dimers in a crossed optical dipole trap, and a study of the BEC-BCS crossover region. Unlike all previous observations of molecular BEC made in single beam dipole traps with very elongated geometries, our condensates are formed in nearly isotropic strongly confining

traps. The experimental setup has been described previously [12, 13]. A gas of ^{6}Li atoms is prepared in the absolute ground state $|1/2, 1/2\rangle$ in a Nd-YAG crossed beam optical dipole trap. The horizontal beam (resp. vertical) propagates along x (y), has a maximum power of $P_o^h = 2\,\mathrm{W}$ ($P_o^v = 3.3\,\mathrm{W}$) and a waist of $\sim 25\,\mu\mathrm{m}$ ($\sim 40\,\mu\mathrm{m}$). At full power, the ^{6}Li trap oscillation frequencies are $\omega_x/2\pi = 2.4(2)\,\mathrm{kHz}$, $\omega_y/2\pi = 5.0(3)\,\mathrm{kHz}$, and $\omega_z/2\pi = 5.5(4)\,\mathrm{kHz}$, as measured by parametric excitation, and the trap depth is $\sim 80\,\mu\mathrm{K}$. After sweeping the magnetic field B from 5 G to 1060 G, we drive the Zeeman transition between $|1/2, 1/2\rangle$ and $|1/2, -1/2\rangle$ with a 76 MHz RF field to prepare a balanced mixture of the two states. As measured recently [11], the Feshbach resonance between these two states is peaked at 834(2) G, and for B=1060 G, $a = -167\,\mathrm{nm}$. After 100 ms the coherence between the two states is lost and plain evaporation provides $N_\uparrow = N_\downarrow = N_{\mathrm{tot}}/2 = 1.5 \times 10^5$ atoms at $10\,\mu\mathrm{K}$=0.8 T_{F}, where $k_{\mathrm{B}} T_{\mathrm{F}} = \hbar^2 k_{\mathrm{F}}^2/2m = \hbar(3N_{\mathrm{tot}}\omega_x\omega_y\omega_z)^{1/3} = \hbar\bar{\omega}(3N_{\mathrm{tot}})^{1/3}$ is the Fermi energy. Lowering the intensity of the trapping laser to 0.1 P_0, the Fermi gas is evaporatively cooled to temperatures T at or below $0.2\,T_{\mathrm{F}}$ and $N_{\mathrm{tot}} \approx 7 \times 10^4$.

Then, sweeping the magnetic field to 770 G in 200 ms, the Feshbach resonance is slowly crossed. In this process atoms are adiabatically and reversibly transformed into cold molecules [13, 14] near the BEC critical temperature as presented in figure 1a. The onset of condensation is revealed by bimodal and anisotropic momentum distributions in time of flight expansions of the molecular gas. These images are recorded as follows. At a fixed magnetic field, the optical trap is first switched off. The cloud expands typically for 1 ms and then the magnetic field is increased by 100 G in 50 μs. This converts the molecules back into free atoms above resonance without releasing their binding energy [3]. Switching the field abruptly off in 10 μs, we detect free ^{6}Li atoms by light absorption near the D2 line. We have checked that, in the trap before expansion, there are no unpaired atoms. In figure 1b, a Bose-Einstein condensate of ^{7}Li atoms produced in the same optical trap is presented. The comparison between the condensate sizes after expansion dramatically reveals that the mean field interaction and scattering length are much larger for ^{6}Li$_2$ dimers (Fig. 1a) than for ^{7}Li atoms (Fig. 1b).

To measure the molecule-molecule scattering length, we produce pure molecular condensates by taking advantage of our crossed dipole trap. We recompress the horizontal beam to full power while keeping the vertical beam at the low power of 0.035 P_0^v corresponding to a trap depth for molecules $U = 5.6\,\mu\mathrm{K}$. Temperature is then limited to $T \leq 0.9\,\mu\mathrm{K}$ assuming a conservative $\eta = U/k_{\mathrm{B}}T = 6$, whereas the critical temperature increases with the mean oscillation frequency. Consequently, with an axial (resp. radial) trap frequency of 440 Hz (resp. 5 kHz), we obtain $T/T_{\mathrm{C}}^0 \leq 0.3$, where $T_{\mathrm{C}}^0 = \hbar\bar{\omega}(0.82N_{\mathrm{tot}}/2)^{1/3} =2.7\,\mu\mathrm{K}$ is the non interacting BEC critical temperature. Thus, the condensate should be pure as confirmed by our images. After 1.2 ms of expansion, the radius of the condensate in the x (resp. y) direction is $R_x = 51\,\mu\mathrm{m}$ ($R_y = 103\,\mu\mathrm{m}$). The resulting anisotropy $R_y/R_x = 2.0(1)$ is consistent with the value 1.98 [15] predicted the scaling equations [16, 17]. Moreover, this set of equation leads to an *in-trap* radius $R_x^0 = 26\mu\mathrm{m}$ (resp. $R_y^0 = 2.75\mu\mathrm{m}$). We then deduce the molecule-molecule scattering length from the Thomas-Fermi formula $R_{x,y}^0 = a_{\mathrm{ho}}\bar{\omega}/\omega_{x,y}(15N_{\mathrm{tot}}a_{\mathrm{m}}/2a_{\mathrm{ho}})^{1/5}$, with $a_{\mathrm{ho}} = \sqrt{\hbar/2m\bar{\omega}}$. Averaging over several images, this yields a_{m} =170$^{+100}_{-60}$ nm at 770 G. Here, the statistical uncertainty is negligible compared to the systematic uncertainty due to the calibration of our atom number. At this field, we calculate an atomic scattering length of $a = 306\,\mathrm{nm}$. Combined with the prediction $a_{\mathrm{m}} = 0.6\,a$ of [18], we obtain $a_{\mathrm{m}} = 183\,\mathrm{nm}$ in good

agreement with our measurement. For ^{7}Li, we obtain with the same analysis a much smaller scattering length of $a_7 = 0.65(10)$ nm at 610 G also in agreement with theory [19].

The condensate lifetime is typically $\sim$300 ms at 715 G ($a_{\rm m} = 66$ nm) and $\sim$3 s at 770 G ($a_{\rm m} = 170$ nm), whereas for $a = -167$ nm at 1060 G, the lifetime exceeds 30 s. On the BEC side, the molecule-molecule loss rate constant is $G = 0.26^{+0.08}_{-0.06} \times 10^{-13}$ cm^3/s at 770 G and $G = 1.75^{+0.5}_{-0.4} \times 10^{-13}$ cm^3/s at 715 G with the fit procedure for condensates described in [20]. Combining similar results for four values of the magnetic field ranging from 700 G to 770 G, we find $G \propto a^{-1.9\pm0.8}$ (figure 2). Our data are in agreement with the theoretical prediction $G \propto a^{-2.55}$ of ref. [18] and with previous measurements of G in a thermal gas at 690 G [13] or in a BEC at 764 G [6]. A similar power law was also found for ^{40}K [21].

We then made an investigation of the crossover from a Bose-Einstein condensate to an interacting Fermi gas (Fig. 1.c and d). We prepare a nearly pure condensate with 3.5×10^4 molecules at 770 G and recompress the trap to frequencies of $\omega_x = 2\pi \times 830$ Hz, $\omega_y = 2\pi \times 2.4$ kHz, and $\omega_z = 2\pi \times 2.5$ kHz. The magnetic field is then slowly swept at a rate of 2 G/ms to various values across the Feshbach resonance. The 2D momentum distribution after a time of flight expansion of 1.4 ms is then detected as previously. As B increases from the regime of weak interactions the condensate size gradually increases towards the width of a non interacting Fermi gas. Nothing particular happens on resonance. Fig. 1.c and 1.d present respectively the anisotropy of the cloud after expansion η and the corresponding released energy $E_{\rm rel}$. These are calculated from gaussian fits to the density after time of flight: $E_{\rm rel} = m(2\sigma_y^2 + \sigma_x^2)/2\tau^2$ and $\eta = \sigma_y/\sigma_x$, where σ_i is the rms width along i, and τ is the time of flight. The anisotropy monotonically decreases from $\sim$1.6 on the BEC side, where hydrodynamic expansion predicts 1.75, to 1.1, at 1060 G, on the BCS side. On resonance, at zero temperature, a superfluid hydrodynamic expansion is expected [22] and would correspond to $\eta = 1.7$. We find however $\eta = 1.35(5)$, indicating a partially hydrodynamic behavior that could be due to a reduced superfluid fraction. On the $a < 0$ side, the decreasing anisotropy would indicate a further decrease of the superfluid fraction that could correspond to the reduction of the condensed fraction of fermionic atom pairs away from resonance observed in [7, 8]. Interestingly, our results differ from that of ref.[23] where hydrodynamic expansion was observed at 910 G in a more elongated trap for $T/T_{\rm F} \simeq 0.1$.

In the BEC-BCS crossover regime, the gas energy released after expansion $E_{\rm rel}$ is also smooth (Fig. 1.d). $E_{\rm rel}$ presents a plateau for $B \leq 750$ G, and then increases monotonically towards that of a weakly interacting Fermi gas. The plateau is not reproduced by the mean field approach of a pure condensate (dashed line). This is a signature that the gas is not at $T = 0$. It can be understood with the mean field approach we used previously to describe the behavior of the thermal cloud. Since the magnetic field sweep is slow compared to the gas collision rate [13], we assume that this sweep is adiabatic and conserves entropy [24]. We then adjust this entropy to reproduce the release energy at a particular magnetic field, $B = 720$ G. The resulting curve as a function of B (solid line in Fig. 1.d) agrees well with our data in the range 680 G $\leq B \leq$ 770 G, where the condensate fraction is 40%, and the temperature is $T \approx T_{\rm C}^0/2 = 1.4\,\mu$K. This model is limited to $n_m a_{\rm m}^3 \lesssim 1$. Near resonance the calculated release energy diverges and clearly departs from the data. On the BCS side, the release energy of a $T = 0$ ideal Fermi gas gives an upper bound for the data (dot-dashed curve), as expected from negative interaction energy and a very

cold sample. This low temperature is supported by our measurements on the BEC side and the assumption of entropy conservation through resonance which predicts $T = 0.1\, T_{\mathrm{F}}$ on the BCS side [24].

On resonance the gas is expected to reach a universal behavior, as the scattering length a is not a relevant parameter any more [25]. In this regime, the release energy scales as $E_{\mathrm{rel}} = \sqrt{1 + \beta} E^0_{\mathrm{rel}}$, where E^0_{rel} is the release energy of the non-interacting gas and β is a universal parameter. From our data at 820 G, we get $\beta = -0.64(15)$. This value is larger than the Duke result $\beta = -0.26 \pm 0.07$ at 910 G [23], but agrees with that of Innsbruck $\beta = -0.68^{+0.13}_{-0.10}$ at 850 G [6], and with the most recent theoretical prediction $\beta = -0.56$ [26, 27]. Around 925 G, where $a = -270\,\mathrm{nm}$ and $(k_{\mathrm{F}}|a|)^{-1} = 0.35$, the release energy curve displays a change of slope. This is a signature of the transition between the strongly and weakly interacting regimes. It is also observed near the same field in [6] through *in situ* measurement of the trapped cloud size. Interestingly, the onset of resonance condensation of fermionic atom pairs observed in ^{40}K [7] and ^{6}Li [8], corresponds to a similar value of $k_{\mathrm{F}}|a|$.

2 P-wave resonances

Recently, both experimental [28, 29, 30] and theoretical [31] papers have devoted interest to the p-wave Feshbach resonances. The goal of these experiments is to nucleate molecules with internal angular momentum $l = 1$, that could lead to the observation of some non-conventional superconductivity, analogous to that observed in superfluid ^{3}He [32].

In the manifold $f = 1/2$ corresponding to the hyperfine ground state of ^{6}Li, coupled channels calculations have demonstrated that three Feshbach resonances could be observed in p-wave channels. The position of the resonances are calculated using the most recent experimental data available on ^{6}Li and are presented in Tab. 1. The predicted values of the resonance position are compared with the location we obtained experimentally using the following procedure: we prepare ^{6}Li atoms in the dipole trap with the required spin state (m_f, m'_f) using radiofrequency transfer. We then ramp up the magnetic field from 0 to a value B_1 slightly higher than the predicted position of the Feshbach resonance. The magnetic field is then abruptly decreased to a variable value B close to resonance. After a waiting time of 50 ms in the trap, we measure the atom number by time of flight imaging. In Fig. 3.a, we show the evolution of the atom number vs magnetic field in the channel (1/2,-1/2). We observe a sharp decrease of the atom number at ~ 186.5 G, close to the predicted value 185 G. The two other channels display similar losses in the vicinity of the theoretical position of the Feshbach resonances (Tab. 1). Note that in this table the experimental uncertainty is mainly due to the magnetic field calibration.

One of the main issue of the physics of Feshbach resonances is related to the lifetime of the molecules, and more generally of the atoms, at resonance. Indeed, one of the key element that led to the experiments on the BEC-BCS crossover was the increase of the lifetime of molecules composed of fermions close to resonance. To address this issue, we have measured the time evolution of the atom number N in the sample at the three Feshbach resonances. Since the one-body lifetime is ~ 30 s, much longer than the measured decay time (~ 100 ms), we can fit the time evolution using the rate equation

(m_{f_1}, m_{f_2})	B_{th} G	B_{exp} G	K cm$^3 \cdot \mu$K$\cdot$s^{-1}	γ μK	μ μK$\cdot$G^{-1}
(1/2,1/2)	159	160.2(6)	–	–	–
(1/2,-1/2)	185	186.2(6)	1.21×10^{-13}	0.05	117
(-1/2,-1/2)	215	215.2(6)	7.33×10^{-13}	0.08	111

Table 1: Position and two-body losses parameters of the p-wave Feshbach resonances of ^{6}Li atoms in $|f_1 = 1/2, m_{f_1}\rangle$ and $|f_2 = 1/2, m_{f_2}\rangle$.

$$\frac{\dot{N}}{N} = -G_2\langle n\rangle - L_3\langle n^2\rangle, \tag{1}$$

where n is the atom density and $\langle n^a\rangle = \int \mathrm{d}^3r\, n^{a+1}/N$ $(a = 1, 2)$ is calculated from the classical Boltzman distribution.

In contrast to s-wave Feshbach resonances where dipolar losses are forbidden in the $f = 1/2$ manifold [33], the losses near a p-wave resonance are found to be dominantly 2-body in the (1/2,-1/2) and (-1/2,-1/2) channels. The variations of the 2-body loss rate with temperature are displayed in Fig. 3.c and show very different behaviors in these two channels. This non trivial dependence is actually not the consequence of some specific property of the states involved (eg., the quantum statistics) but can be recovered using a very simple three-state model. We describe inelastic processes by two non interacting open channels, respectively the incoming and decay channels, that are coupled to a single p-wave molecular state . This model leads to a very simple algebra that can be treated analytically [34] and yields for the two-body loss-rate at a given energy E

$$g_2(E) = \frac{KE}{(E - \delta)^2 + \gamma^2/4}. \tag{2}$$

Here $\delta = \mu(B - B_F)$ is the detuning to the Feshbach resonance and K, μ and γ are phenomenological constants depending on the microscopic details of the potential. For each channel, these parameters are estimated from our numerical coupled-channel calculation (Tab. 1).

Eqn. (2) shows that, contrarily to s-wave processes that can be described accurately by their low energy behavior, p-wave losses are dominated by the resonance peak located at $E = \delta$ where the losses are maximum. In other word, the so-called "threshold laws", that give the low energy scattering behavior, are insufficient to describe a Feshbach resonance associated with p-wave molecular states (and, more generally, any non zero angular momentum molecular state).

To compare with experimental data, Eq. (2) is averaged over a thermal distribution and for $\delta > 0$ and $\delta \gg \gamma$ we get:

$$G_2 \sim 4\sqrt{\pi}\frac{K}{\gamma}\left(\frac{\delta}{k_B T}\right)^{3/2}\mathrm{e}^{-\delta/k_B T}. \tag{3}$$

Eqn. 3 is used to fit the data of Fig. 3.b, with $B - B_F$ as the only fitting parameter. We get a fairly good agreement if we take $B - B_F = 0.04$ G (resp. 0.3 G) for the (-1/2,-1/2) (resp. (1/2,-1/2)) channel, illustrating the extreme sensitivity of G_2 to detuning and temperature. This feature was also tested by measuring the variations of G_2 with

magnetic field at constant temperature. Note that the width of the resonance, as given by Eqn. 3, is of the order of $k_\mathrm{B}T/\mu$. At $\sim 10\,\mu$K, this yields a width of ~ 0.1 G, which is comparable with the one observed in Fig. 3.a.

In the $(1/2,1/2)$ channel, dipolar losses are forbidden and we indeed find that 3-body losses are dominant. The dependence of L_3 with temperature is very weak (Fig. 3.b) and contradicts the low energy theoretical calculation of the temperature dependence of three-body loss rate performed in [35]. Indeed, Wigner threshold law predicts that at low energy, L_3 should be proportional to T^λ, with $\lambda \geq 2$ for indistinguishable fermions. However, as we noticed earlier in the case of two-body losses, the threshold law is probably not sufficient to describe losses at resonance due to the existence of a resonance peak that might also be present in three-body processes. This suggests that 3-body processes must be described by a more refined formalism, analogous to the unitary limited treatment of the s-wave elastic collisions [36].

Finally, we have checked the production of molecules in $(1/2,-1/2)$ mixture by using the scheme presented in [13, 14]. We first generate p-wave molecules by ramping in 20 ms the magnetic field from 190 G $> B_\mathrm{F}$ to $B_\mathrm{nuc} = 185$ G $< B_\mathrm{F}$. At this stage, we can follow two paths before detection. Path 1 permits to measure the number N_1 of free atoms: by ramping *down* in 2 ms the magnetic field from 185 G to 176 G, we convert the molecules into deeply bound molecular states that decay rapidly by 2-body collisions. Path 2 gives access to the total atom number N_2 (free atoms + atoms bound in p-wave molecules). It consists in ramping *up* the magnetic field in 2 ms from B_nuc to 202 G $> B_\mathrm{F}$ to convert the molecules back into atoms. Since the atoms involved in molecular states appear only in pictures taken in path 2, the number of molecules in the trap is $(N_2 - N_1)/2$. In practice, both sequences are started immediately after reaching B_nuc and we average the data of 25 pictures to compensate for atom number fluctuations. We then get $N_1 = 7.1(5) \times 10^4$ and $N_2 = 9.1(7) \times 10^4$ which corresponds to a molecule fraction $1 - N_1/N_2 = 0.2(1)$. Surprisingly, we failed to detect any molecule signal when applying the same method to $(1/2,1/2)$ atoms.

3   Heteronuclear Feshbach resonances

So far, the Feshbach resonances used in this paper were involving atoms of the same species (namely ^{6}Li). However, it was recently pointed out that the observation of Feshbach resonances between two different atom species could lead to a host of interesting effects ranging from the observation of supersolid order [37] to the study polar molecules [38]. In the case of a mixture of bosons and fermions, these molecules are fermions and are expected to be long lived. Indeed, Pauli principle keeps molecules far apart and prevents inelastic collisions. Such resonances were observed experimentally in ^{6}Li-^{23}Na [39] and ^{40}K-^{87}Rb [40] mixtures. In the case of ^{6}Li-^{7}Li in the stable Zeeman ground state $|f = 1/2, m_f = 1/2\rangle \otimes |f = 1, m_f = 1\rangle$, the existence and the position of heteronuclear Feshbach resonances were predicted in [41]. In that work, the ^{6}Li-^{7}Li interaction potential was extracted from the data on ^{6}Li-^{6}Li scattering properties by mean of a simple mass-scaling. Using coupled channels calculation it was found that this system exhibited five Feshbach resonances whose position is displayed in Tab. 2 [42].

Experimentally, we probed these Feshbach resonances using a mixture of respectively $N_6 \sim N_7 \sim 10^5$ atoms of ^{6}Li and ^{7}Li in the absolute Zeeman ground state $|1/2, 1/2\rangle \otimes |1, 1\rangle$. The gas is cooled at a temperature of $4\,\mu$K in the cross dipole

B_{th} (G)	B_{exp} (G)
218	not seen
230	226.3(6) G
251	246.0(8) G
551	539.9(8) G
559	548.6(9) G

Table 2: Predicted and observed positions of the heteronuclear Feshbach resonances of a ^{6}Li-^{7}Li gas. First column: resonance position as predicted by coupled channel calculation. Secund column: experimental determination of the resonances. The experimental error bars are due to the systematic uncertainty on the calibration of the magnetic field. The first Feshbach resonance is extremely narrow and could not be detected with our experimental resolution.

trap and we locate the resonance by sweeping down in 1 s the magnetic field from a value located about 20 G above the predicted position of the resonance to a variable value B. By looking for the value of B at which we start loosing atoms, we were able to detect four of the five resonances at a value very close to that predicted by theory (Tab. 2). The discrepancy between the experimental and theoretical values is larger in this case than in the case of th p-wave resonance. This is probably due to a breakdown of the Born-Oppenheimer approximation that one expects in the case of light atoms such as lithium and that forbids the use of the mass scaling [41]. Note also that the missing resonance is predicted to be very narrow ($\sim$1 mG).

As noticed in [43], the width of a Feshbach resonance strongly influences the molecule lifetime that can be much higher close to a wide resonance. Since the Feshbach resonances we found in $|1/2, 1/2\rangle \otimes |1, 1\rangle$ are very narrow (~ 0.1 G) it might prove interesting to look for wider Feshbach resonances. In the case of ^{6}Li-^{7}Li, a wide resonance is predicted to exist in the stable state $|3/2, 3/2\rangle \otimes |1, 1\rangle$ at ~ 530 G, in agreement with our observation of a large atom loss located between ~ 440 G and ~ 540 G.

References

[1] M. Greiner, C. A. Regal, and D. S Jin, Nature **426**, 537 (2003).

[2] S. Jochim *et al.*, Science **302**, 2101 (2003).

[3] M. W. Zwierlein *et al.*, Phys. Rev. Lett. **91**, 250401 (2003).

[4] T. Bourdel *et al.*, Phys. Rev. Lett. **93**, 050401 (2004)

[5] A.J. Leggett, J. Phys. C. (Paris) **41**,7 (1980); P. Nozières and S. Schmitt-Rink, J. Low Temp. Phys. **59** 195 (1985); C. Sá de Melo, M. Randeria, and J. Engelbrecht, Phys. Rev. Lett. **71**, 3202 (1993); M. Holland, S. Kokkelmans, M. Chiofalo, and R. Walser, Phys. Rev. Lett. **87** 120406 (2001); Y. Ohashi and A. Griffin, Phys. Rev. Lett. **89**, 130402 (2002); J. N. Milstein, S. J. J. M. F. Kokkelmans, and M. J. Holland, Phys. Rev. A **66**, 043604 (2002); R. Combescot, Phys. Rev. Lett. **91**, 120401 (2003); G. M. Falco and H. T. C. Stoof, cond-mat/0402579.

[6] M. Bartenstein *et al.*, Phys. Rev. Lett. **92**, 120401 (2004).

[7] C. A Regal, M. Greiner, and D. S. Jin Phys. Rev. Lett. **92**, 040403 (2004).

[8] M. Zwierlein *et al.*, Phys. Rev. Lett. **92**, 120403 (2004).

[9] M. Greiner *et al.*, e-print cond-mat/0407381.

[10] J. Kinast *et al.*, Phys. Rev. Lett. *92*, 150402 (2004)

[11] C. Chin *et al.*, Science **305**, 1128 (2004).

[12] T. Bourdel *et al.*, Phys. Rev. Lett. **91**, 020402 (2003).

[13] J. Cubizolles *et al*, Phys. Rev. Lett. **91** 240401 (2003).

[14] C. A. Regal, C. Ticknor, J. L. Bohn, and D. S. Jin, Nature **424**, 47 (2003).

[15] We correct our data for the presence of a magnetic field curvature which leads to an anti-trapping frequency of 100 Hz at 800 G along x.

[16] Yu. Kagan, E. L. Surkov, and G. V. Shlyapnikov, Phys. Rev. A **54**, R1753 (1996).

[17] Y. Castin and R. Dum, Phys. Rev. Lett. **77**, 5315 (1996).

[18] D. S. Petrov, C. Salomon, and G. V. Shlyapnikov, Phys. Rev. Lett. **93**, 090404 (2004).

[19] L. Khaykovich *et al.*, Science **296**, 1290 (2002).

[20] J. Söding, *et al*, Applied Physics **B69**, 257 (1999)

[21] C. Regal, M. Greiner and D. Jin, Phys. Rev. Lett. **92**, 083201 (2004).

[22] C. Menotti, P. Pedri, and S. Stringari, Phys. Rev. Lett. **89**, 250402 (2002).

[23] K. O'Hara *et al.*, Science **298**, 2179 (2002). M. Gehm *et al.*, Phys. Rev. A **68**, 011401 (2003).

[24] L. D. Carr, G. V. Shlyapnikov, and Y. Castin, cond-mat/0308306.

[25] H. Heiselberg, Phys. Rev. A **63**, 043606 (2001).

[26] J. Carlson, S.Y. Chang, V. R. Pandharipande, and K. E. Schmidt, Phys. Rev. Lett. **91**, 050401 (2003).

[27] G. E. Astrakharchik, J. Boronat, J. Casulleras, and S. Giorgini, cond-mat 0406113 (2004).

[28] C. A. Regal, C. Ticknor, J. L. Bohn, and D. S. Jin Phys. Rev. Lett. **90**, 053201 (2003).

[29] J. Zhang *et al.*, Phys. Rev. A **70**, 030702 (2004)

[30] C. H. Schunck *et al.*, e-print cond-mat/0407373.

[31] T.L. Ho and N. Zahariev, e-print cond-mat/0408469; T.L. Ho and R.B. Diener, e-print cond-mat/0408468.

[32] D. M. Lee, Rev. Mod. Phys. **69**, 645 (1997).

[33] K. Dieckmann *et al.*, Phys. Rev. Lett. **89**, 203201 (2002).

[34] F. Chevy *et al.*, to be published.

[35] B. D. Esry, C. H. Greene, and H. Suno, Phys. Rev. A **65**, 010705 (2002).

[36] H. Suno, B. D. Esry, and C. H. Greene, Phys. Rev. Lett. 90, 053202 (2003).

[37] H.P. Büchler and G. Blatter, Phys. Rev. Lett. **91**,130404 (2003).

[38] M.A. Baranov, M.S. Mar'enko, V.S. Rychkov and G. Shlyapnikov, Phys. Rev. A **66** 013606 (2002).

[39] C.A. Stan *et al.*, Phys. Rev. Lett. **93**, 143001 (2004).

[40] S. Inouye *et al.*, e-print cond-mat/0406208.

[41] E.G.M. van Kempen, B. Marcellis and S.J.J.M.F Kokkelmans, e-print cond-mat/0406722.

[42] Note that the absence of symmetrization constraint in the case of a heteronuclear system allows for many more resonances than for a pure system.

[43] R. Combescot, Phys. Rev. Lett. **91**, 120401 (2003); G.M. Bruun and C. J. Pethick, Phys. Rev. Lett. **92**, 140404 (2004).
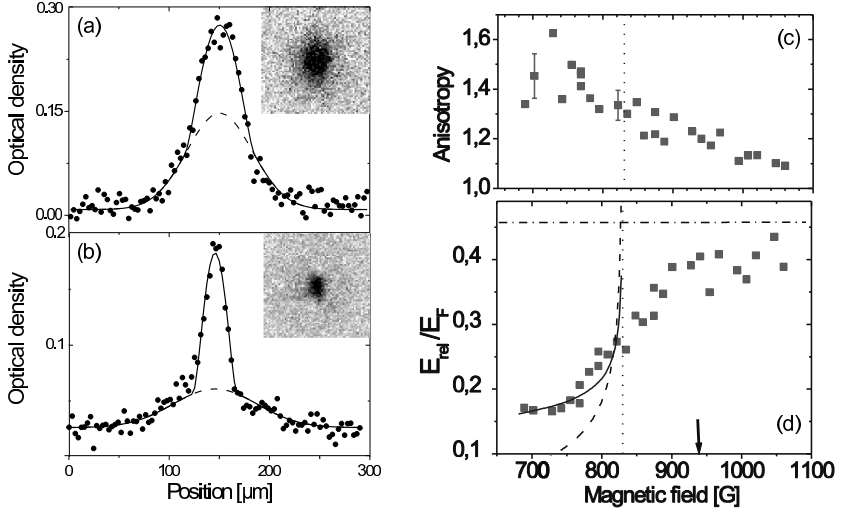
Figure 1: a,b: Onset of Bose-Einstein condensation in a cloud of 2×10^4 ^{6}Li dimers at $770\,\mathrm{G}$ (a) and of 2×10^4 ^{7}Li atoms at $610\,\mathrm{G}$ (b) in the same optical trap. (a): $1.2\,\mathrm{ms}$ expansion profiles along the weak direction x of confinement. (b): $1.4\,\mathrm{ms}$ expansion. The different sizes of the condensates reflect the large difference in scattering length $a_\mathrm{m} = 170\,\mathrm{nm}$ for ^{6}Li dimers and $a_7 = 0.55\,\mathrm{nm}$ for ^{7}Li. Solid line: Gaussian+Thomas-Fermi fit. Dashed line: gaussian component. Condensate fractions are $44\,\%$ in (a) and 28% in (b). c,d: BEC-BCS crossover. (c): anisotropy of the cloud. (d): release energy across the BEC-BCS crossover region. In (d), the dot-dashed line corresponds to a $T = 0$ ideal Fermi gas. The dashed curve is the release energy from a pure condensate in the Thomas-Fermi limit. The solid curve corresponds to a finite temperature mean field model with $T = 0.5\,T_\mathrm{C}^0$. Arrow: $k_\mathrm{F}|a| = 3$.
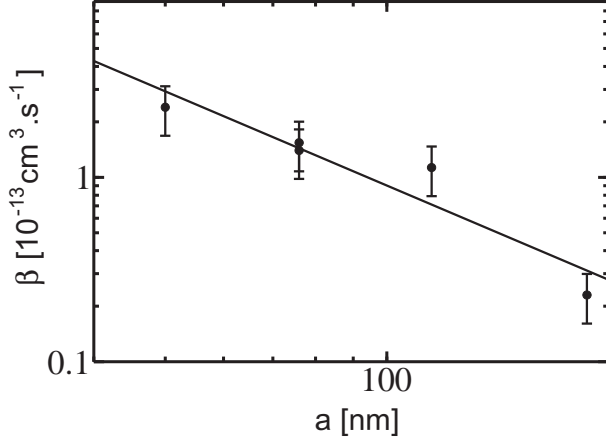
Figure 2: Molecular condensate loss rate β as a function of the atomic scattering length a near the 834 G s-wave Feshbach resonance. The line is a power law fit with $\beta \sim a^{-1.9\pm0.8}$ in agreement with theory, $\beta \sim a^{-2.55}$ [18].
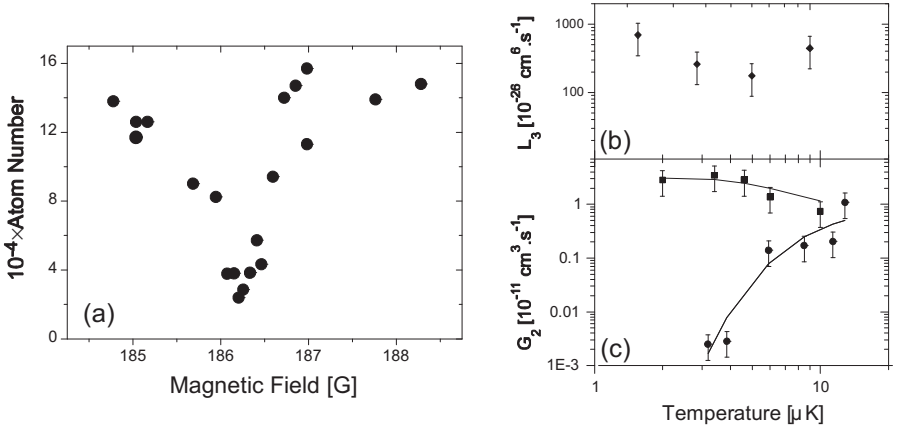

Figure 3: (a) Atom number vs. magnetic field $B_{0,f}$ after a 50 ms wait for atoms in the spin mixture $(1/2, -1/2)$ at $T \sim 14\mu K$. The sharp drop close to $B_0 \sim 186$ G over a range $\simeq 0.5$ G is the signature of the p-wave Feshbach resonance predicted by theory. (b) (resp. (c)) Variations of 3-body (2-body) loss rates vs temperature at the Feshbach resonance. (b): ♦: atoms in the Zeeman ground state $|f = 1/2, m_f = 1/2\rangle$, $B_{0,f} \sim 159$ G. (c): ■: atoms polarized in $|f = 1/2, m_f = -1/2\rangle$, $B_{0,f} \sim 215$ G. ●: mixture $|f = 1/2, m_f = 1/2\rangle + |f = 1/2, m_f = -1/2\rangle$, $B_{0,f} \sim 186$ G. In both cases, the full line is a fit to the data using prediction of Eq. 3 with the magnetic field as the only fitting parameter.